

# Waveguide Microchannel Crossing for Terahertz Spectroscopy

Guillermo Oviedo Vela<sup>1</sup> and Mark S. Miller<sup>1,2</sup>

<sup>1</sup>Electrical & Computer Engineering Department

<sup>2</sup>Materials Science & Engineering, University of Utah

## Abstract

The large attenuation of terahertz radiation in water greatly complicates far infrared spectroscopy of aqueous species. The device developed in this work enables terahertz aqueous spectroscopy by intersecting a waveguide with a micro-fluidic channel. An overview of the process involved to fabricate such a device is presented. Measured transmission, simulated transmission, simulated structural and simulated fluidic data is also presented. The ultimate goal of this device is to be implemented in miniaturized spectroscopy systems, such as lab-on-chip integration.

**Keywords:** Terahertz, Waveguide, Microchannel, Spectroscopy, Far infrared, PDMS, micro-fluidics.

## 1 Introduction

The 80 dB per centimeter absorption of water at 2.5 THz, for example, requires that samples for spectroscopy be thin. Far infrared spectra of aqueous chemical and biomolecular species have generally not been reported. One of the few reports of terahertz spectroscopy of biological samples includes spectra taken from dry, thin samples of DNA [1]. The waveguide microfluidic-channel crossing (WaMiX) device presented here should enable convenient aqueous sample introduction and far infrared spectroscopy [2]. Figure 1 shows the geometry of the cross device at the intersection and gives the simulated result of a terahertz wave propagating through the device. The design issues that arise from integrating such a device include minimizing electromagnetic losses, matching the cross impedance to the waveguide, and developing the microfabrication processes. The following sections present the design choices taken along with the electromagnetic, microfluidic, and mechanical simulations that support them. Far infrared transmission measurements are finally presented and discussed.

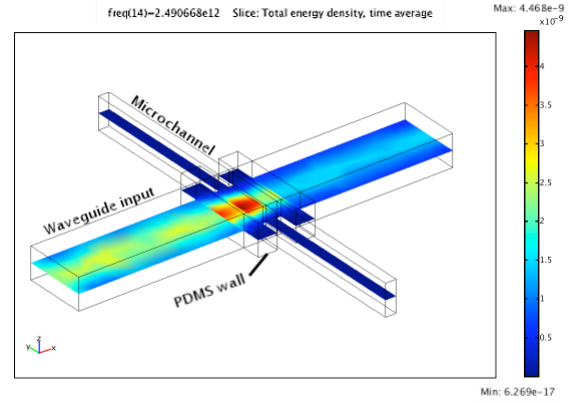


Figure 1: Dissipation through microfluidic channel with reduced channel width and quarter-wave transformer PDMS walls.

## 2 Device design

The overall design approach uses rectangular waveguides and microfluidic channels that are simultaneously etched into a silicon substrate. As depicted in Fig. 1 polydimethyl siloxane (PDMS) walls seal the channel from the waveguide. The PDMS wall thickness and matching stubs and microchannel width are chosen to match the cross impedance to the waveguide. The microchannel width is constrained not only to reduce absorption, but also to give a high frequency cut-off that prevents terahertz propagation in the channel. Terahertz coupling into the waveguide was accomplished through the implementation of silicon micromachined horn antennas [3].

### 2.1 Waveguide losses

The dominant electromagnetic loss mechanisms in terahertz waveguides are conduction and dielectric losses. Waveguide structures provide mechanisms for radiation coupling and propagation with low conduction loss [4]. Micromachining techniques are ways in

which researchers have implemented structures suitable for terahertz system integration [5]. The present device uses the lowest transverse electric field mode (TE<sub>10</sub>) which has the lowest loss due to conductor losses. The waveguide design parameters used to design the waveguide have been taken from Pozar' [6] and Balanis [7].

The conductor losses for the gold coated waveguides were accounted for by using a gold conductivity of  $4.1 \times 10^7$  S/cm. A Debye approximation was used to estimate the relative dielectric constant of water, including loss [7, 8]. At 2.5 THz it is calculated to be  $\epsilon_r = (5.2 + i.56)\epsilon_0$ , where  $\epsilon_0$  is the permittivity of air. The dielectric properties of water vapor were not taken into account in this work. Since the proposed device required the integration of windows to prevent fluid from traveling down the waveguide, the EM loss through window materials was considered. Material loss information at terahertz frequencies is available for a limited amount of materials. Some of the window materials investigated in the literature were polyethylene, quartz and silicon [9]. Windows made of polyethylene or quartz were not considered because their integration to the fabrication of the device would require further process development. Silicon was determined not to be appropriate for the application, because although silicon windows can be left between the waveguide and the channel, losses into the substrate were unacceptably high. Fourier transform spectrometry (FTS) measurements were performed to determine the dielectric properties of PDMS, which is commonly used in microfluidics, and an attenuation of 33% was found for a  $940\mu\text{m}$  of PDMS.

## 2.2 Micro-fluidic flow conditions

Two mechanisms are commonly implemented to move the fluid in microfluidic channels, namely capillarity forces and induced pressure. As the channel dimensions shrink, high inlet pressures are required to produce flow, which can generate leaks at interfaces, such as the interface between the body and the lid of the channel present in this device. PDMS gaskets were used to prevent interface leaks and form windows for radiation to go through. Induced pressure in microchannels can be applied using different pumping schemes. A 27 picoliter cavity was implemented to form a volume that contains the sample. At a characteristic flow velocity of 0.1 mm/s, the sample volume changes over approximately 1.2 seconds.

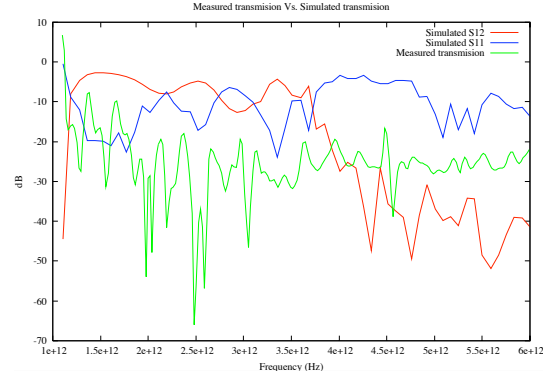


Figure 2: S12, S11 and measured power transmission through structure with channel and quarter-wave transformer PDMS walls.

## 3 Modelling

### 3.1 Electromagnetic simulations

Simulations were performed to understand the attenuation processes of the waveguide-microchannel crossing. The assumptions made for the simulations include ideal coupling of the TE<sub>10</sub> mode of propagation to the waveguide, surfaces with no roughness, perfect corners, vertical walls, and isotropic material properties. The above mentioned assumptions are all potential sources of differences between measured and simulated data. The modeling of the device was performed using commercial finite element method (FEM) software. The conformable properties of tetrahedral elements provide a good first order approximation of the structures, since curved surfaces are neglected. The absence of resonant effects between nodes allows the use of first order elements in the modeling of electromagnetic phenomena.

PDMS matching structures were simulated to minimize the reflections from air-water boundaries. The structure was simulated using several mesh sizes to ensure convergence of the solution. The simulation results are presented in Figures 1 and 2. Figure 1 show the simulated waveguide-microchannel crossing with PDMS walls. The figure graphically shows that no power is being dissipated into the microchannel, but is being concentrated into the spectroscopy volume and further transmitted to the other side of the structure. Figure 2 shows a comparison between the simulated scattering parameters, S11 and S12.

### 3.2 Mechanical simulations

Calculations were performed to learn whether PDMS walls could withstand the pressure required for fluid flow without leaking fluid into the waveguide. For these calculations water was used as the working fluid. Isotropic properties of water were assumed. The highest average velocity used for these calculations was 0.1 mm per second. This velocity is five times the smallest dimension of the channel per second. A  $20\mu\text{m}$  wide by  $480\mu\text{m}$  long microchannel was simulated. At the middle of this channel two boundaries, one on each side of the channel, defined to be  $80\mu\text{m}$  long simulated the presence of the PDMS walls. This geometry was simulated using a mesh of 23000 elements. The Reynold's number of water flowing in the microchannel at the highest velocity is much less than 1 (0.004), predicting laminar flow. The effects of slip conditions at the walls were neglected and the channel was idealized to have no roughness. The pressure profile on the PDMS boundaries resulting from fluid flow at different average input velocities were calculated using second-order triangular La-Grange elements. The resulting pressure profile data was used to calculate the deflection as a function of pressure of the PDMS membrane depicted in Figure 3 (bottom). A mesh of 118000 elements was used to simulated this membrane. The sides of the wall were assumed to be fixed to the substrate. The PDMS modulus of elasticity (7.5 kPa), Poisson's ratio (0.5) and density ( $1050\text{ gr}/\text{m}^3$ ) were taken from manufacturer specifications. Figure 3 shows the deformation of the wall given by the pressure produced from having an average velocity of 0.1 mm/s. The maximum deformation of the PDMS wall observed in this figure is  $0.02\mu\text{m}$  at the face of the wall where direct pressure is applied. This constitutes a deformation of 2%, which is much less than the deformation required for failure specified by the manufacturer (140%). Therefore it was concluded that the PDMS walls would be able to withstand the pressures required for flow in the microchannel.

## 4 Fabrication processes

The following is a brief overview of the relevant bulk micro-machining techniques used for this device. Further information about the bulk micro-machining techniques can be found in the literature [10]

- KOH etching: Potassium hydroxide wet etching was used to create coupling horn antennas and needle inputs.

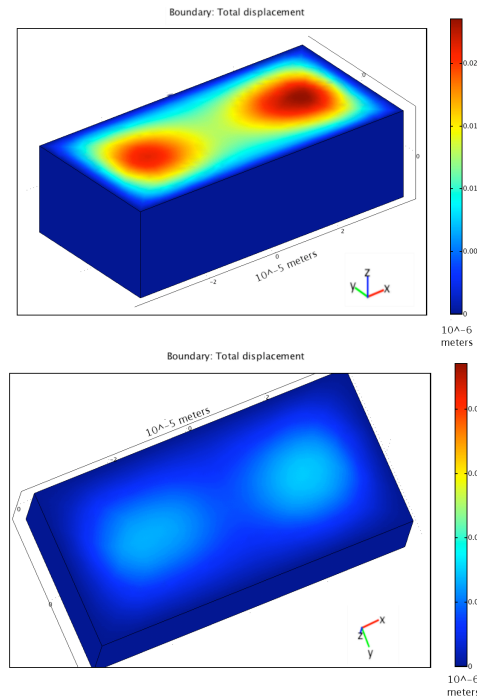


Figure 3: Deformation as a function of pressure of a PDMS wall. Top: Face of the wall where pressure is applied. Bottom: Opposite face.

- RIE etching: Reactive ion etching was used to create the waveguide, microchannels and PDMS windows.
- E-beam evaporation: A coat of gold was deposited upon the fabricated device to minimize attenuation due to silicon absorption.
- Photolithography: Photolithography was used to define all device features and masking layers.
- Packaging: Parts were brought together using PDMS as a gasket and clamped.

Figures 4 and 5 show pictures of the fabricated device prior to be covered with the gold cover lid that finishes the device.

## 5 Far infrared measurements

The device was measured with a Bruker FTIR spectrometer using a globar source, DGTS-FIR detector and T222 beamsplitter. S11 is a measurement of the insertion loss of the device and S12 indicates the calculated transmission through the device. The data presented in figure 2 was taken with nothing but air

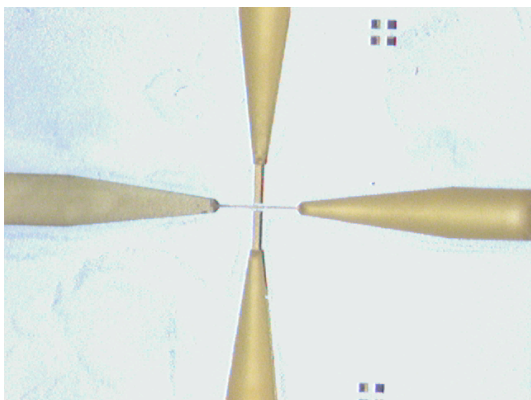


Figure 4: Fabricated device

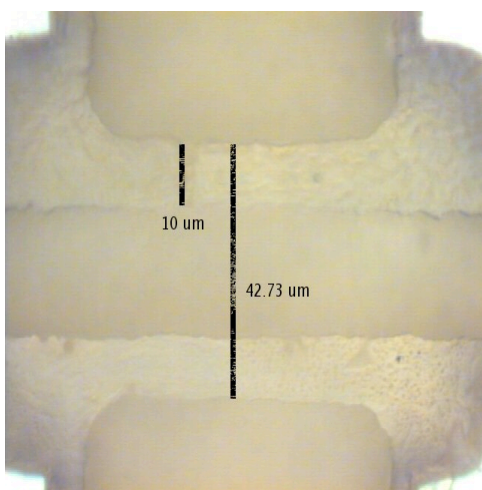


Figure 5: Close-up of spectroscopic volume

in the microchannel. The measurements and simulations presented were made using the actual dimensions of the fabricated device. The final features of the fabricated device lowered the cutoff frequency of the device to approximately 1.1 THz. Atmospheric absorption features modify the measured spectra. To minimize this effect the spectrometer was purged with dry air. The beam splitter was selected because of its transmission window between 30 and 650 wavenumbers.

## 6 Conclusions and future work

The simulations and measurements presented here demonstrate the plausibility of using a WaMiX for aqueous spectroscopy. For gas phase molecules, spectral lines of interest include rotational and vibrational states, which should have analogs in an aqueous environment. The feasibility of using the WaMiX

for spectroscopy will depend on the strength these absorption processes in comparison to other system losses. Future work will include more sensitive transmission spectra of the fabricated devices and transmission spectra of solutions.

## References

- [1] T. R. Globus, "Submillimeter-wave fourier transform spectroscopy of biological macromolecules," *Journal of Applied Physics*, vol. 91, pp. 6105–6113, May 2002.
- [2] G. A. Oviedo, "Terahertz spectroscopy through a micro-channel," Master's thesis, University of Utah, 2004.
- [3] J. L. Hesler, K. Hui, R. K. Dahlstrom, R. M. Weikle, T. W. Crowe, C. M. Mann, and H. B. Wallace, "Analysis of an octagonal micromachined horn antenna for submillimeter-wave applications," *IEEE Transactions on Antennas and Propagation*, vol. 49, pp. 997–1001, June 2001.
- [4] G. Gallot, S. Jamison, R. McGowan, and D. Grishkowsky, "Terahertz waveguides," *J. Opt. Soc.*, vol. 17, pp. 851–863, May 2000.
- [5] V. M. Lubecke, K. Mizuno, and G. M. Rebeiz, "Micromachining for terahertz applications," *IEEE Transactions on Microwave Theory and Techniques*, vol. 46, no. 11, p. 1821, Nov. 1998.
- [6] D. Pozar, *Microwave Engineering*, 2nd ed. USA: John Wiley and Sons, 1998.
- [7] C. A. Balanis, *Advanced Engineering Electromagnetics*, 2nd ed. USA: John Wiley and Sons, 1989.
- [8] "Permittivity (dielectric constant) of water at various frequencies," in *Handbook of Chemistry and Physics*, 85th ed., D. Lide, Ed. CRC Press, 2004-2005.
- [9] D. Koller and G. Ediss, "FTS measurements of some window materials," *Electronics Division Technical Note no. 184*, Aug. 1999.
- [10] M. J. Madou, *Fundamentals of Microfabrication*, 2nd ed. USA: CRC Press, 2002.